ISSN 0036-0244, Russian Journal of Physical Chemistry A, 2016, Vol. 90, No. 1, pp. 122–129. © Pleiades Publishing, Ltd., 2016.
Original Russian Text © S.S. Starodubov, I.V. Nechaev, A.V. Vvedenskii, 2016, published in Zhurnal Fizicheskoi Khimii, 2016, Vol. 90, No. 1, pp. 89–96.

STRUCTURE OF MATTER AND QUANTUM CHEMISTRY

DFT Modeling of Adsorption of Formaldehyde and Methanediol Anion on the (111) Face of IB Metals

S. S. Starodubov, I. V. Nechaev, and A. V. Vvedenskii

Voronezh State University, Voronezh, Russia

e-mail: nechaev_iv@chem.vsu.ru

Received February 12, 2015

Abstract—Gas-phase adsorption of formaldehyde and gas- and liquid-phase adsorption of the methanediol anion on the (111) face of copper, silver, and gold was modeled in terms of the density functional theory and the cluster model of the metal single-crystal surface. In the gas phase, formaldehyde was found to be physically adsorbed on the metals, while the methanediol anion was found to be chemisorbed. It exists on the surface in two different stable states. In aqueous solution, the $H_3CO_2^-$ anion can spontaneously dissociate into the formate ion and two hydrogen atoms.

Keywords: adsorption, dissociative chemisorption, formaldehyde, methanediol anion, quantum-chemical modeling.

DOI: 10.1134/S0036024416010295

INTRODUCTION

Formaldehyde plays an important role in organic synthesis. It is one of the products formed during the oxidation of methanol on the silver surface and is used in industrial synthesis of methanol on the copper surface [1, 2]. At the same time, this is an extremely hazardous contaminant of both gas and liquid media, which can be purified by anodic oxidation among other methods. Metals of IB Subgroup are promising electrode materials in this process because they are much less liable to catalytic poisoning of the surface than platinum. In aqueous solutions, formaldehyde exists as methanediol capable of taking the cation or anion form depending on pH of the medium [3]. From practical viewpoint, the electrooxidation of the methanediol anion in an alkaline medium is more interesting because it occurs at a markedly higher rate than the electrooxidation of the methanediol cation in an acidic medium [4]. Earlier, it was shown by voltammetry, chronoamperometry [5], and labeled atoms method [6] that the adsorption of the methanediol anion on polycrystalline electrodes of gold and silver–gold alloys from aqueous solutions is dissociative and accompanied by the formation of the formate ion. It is not clear whether this conclusion is fully applicable to single-crystal gold, silver, and copper and, which is most important, whether the answer can be found from calculations (using the quantum-chemical procedure of adsorption analysis), but not from rather labor-consuming experiment.

The goal of the present study was to investigate the character of adsorption of the formaldehyde molecule and methanediol anion on the (111) face of Cu, Ag, and Au and to reveal the specific features of the structural and charged state of adsorbate particles on various IB metals using the DFT modeling in the cluster approximation. The (111) face was chosen as an adsorption surface because of its highest percent in the polycrystals of IB metals and also because it is most thermodynamically stable and is less liable to reconstruction under the action of the solvent than other faces [7].

CALCULATION MODEL AND PROCEDURES

The adsorption surface was modeled in the form of a two-layer cluster $Me_{31}(19, 12)$, with a structure of the metal fcc lattice. This model of the crystal surface is widely used for modeling the adsorption processes [8–13]. The interatomic distances in the cluster taken from the experimental data on the lattice parameters of metals [14] were 255.6, 288.9, and 288.4 pm for copper, silver, and gold, respectively. The positions of the metal atoms were fixed in the course of calculations assuming that lattice relaxation induced in the course of adsorption was low.

The calculations were performed in terms of density functional theory (DFT) using the B3LYP hybrid functional [15] (Becke-3 exchange functional combined with the Lee–Yang–Parr nonlocal correlation functional) using the Gaussian-03 program package [16]. The H, C, and O atoms were described using the standard split-valence basis set 6-31G(*d*, *p*) [17]; the LanL2MB pseudopotential with the minimum non-

split basis was used for the Cu, Ag, and Au atoms [18]. Table 1 shows the testing of this calculation scheme on a series of diatomic particles. Regretfully, the use of a more powerful basis set for describing the metal atoms did not lead to convergence for solving the equations of the self-consistent field using Me_{31} clusters. On the other hand, smaller clusters have no sufficient surface for accommodating the adsorption complexes under study. It was decided that exclusion of the interaction of the adsorbate with the angular atoms of the cluster is more important than the use of a more powerful basis set for metal atoms. Note that this calculation scheme was effectively used earlier for modeling the adsorption processes on the metal surface [12], including the modeling of gas-phase adsorption of the methanediol anion in [13]. The obtained energies of H_2CO adsorption on the (111) face of copper and gold differ by no more than 3 and 9 kJ/mol from the corresponding values obtained in [22, 23], where more powerful basis sets LanL2DZ and DNP were used for describing the metal atoms.

Gas-phase adsorption of an X particle on the surface of the Me_{31} cluster is described by the equation

$$Me_{31} + X \rightarrow Me_{31}X. \quad (1)$$

The adsorption energy E_{ads} was calculated as the difference between the total energies of the products and starting substances of process (1). To determine the structures of the adsorption complexes corresponding to the total energy minimum, several variants of initial position of each adsorbate particle on the surface were considered with further geometry optimization using the Berni algorithm [24]. The calculation was carried out with optimization of all the degrees of freedom of the adsorbate atoms.

When modeling the liquid-phase adsorption, which was regarded as replacement-type, it is necessary to take into account not only the presence of H_2O molecules on the surface, but also their desorption, partial dehydration of the adsorbate, and formation of the adsorption complex:

$$Me_{31}(H_2O)_n + X(H_2O)_m \rightarrow Me_{31}X(H_2O)_p + (H_2O)_q. \quad (2)$$

The presence of the solvent was taken into account here within the framework of the molecular model, which suggests direct inclusion of solvent molecules in the calculation procedure. Since the number of H_2O molecules that can be added to the calculation procedure is limited by the size of the cluster surface and the computer resources, the calculations included only the first hydration shell of adsorbate particles and the first adsorption layer of water molecules. Note that the far dielectric environment can generally be included in terms of the continuum model of the solvent, but its use for adsorption on clusters seems doubtful. The reason for this is the fact that when the cluster is surrounded by a medium with bulk dielectric permittivity corresponding to that of the solvent, the field interacts not only with the adsorption surface of the cluster, but also with all other cluster faces. When an adsorbate particle is added, the charges inside the Me_n cluster are redistributed, and the energy of its interaction with the medium changes, which inevitably leads to errors in adsorption energy calculation. In addition, the continuum model neglects the effect of the nonlocal nature of the dielectric response and the presence of an internal phase potential for water [25].

The effective charges on atoms were calculated based on Mulliken population analysis [26]. A frequency analysis was not performed; therefore, all the obtained data should be referred to absolute zero.

Table 1. Calculated and experimental (in parentheses) characteristics of diatomic particles

Particle	D, kJ/mol	R, pm
Cu_2	150.5 (193.9 ± 2.4 [19], 176.52 ± 2.38 [21])	241 (222 [19], 221.97 [21])
Ag_2	114.0 (159.2 ± 2.9 [19], 160.3 ± 3.4 [21])	275 (248 [19], 268 [21])
Au_2	147.9 (220.9 ± 1.9 [19], 226.2 ± 0.5 [21])	268 (247 [19], 247.19 [21])
CuO	224.5 (264 ± 41 [20], 269.0 ± 20.9 [21])	182 (172.46 [20], 172.44 [21])
AgO	142.7 (220.5 ± 14.6 [20], 220.1 ± 20.9 [21])	209 (200.3 [20], 200.30 [21])
AuO	153.4 (225.1 ± 14.6 [20], 221.8 ± 20.9 [21])	198 (184 [20])

RESULTS AND DISCUSSION

Gas-Phase Adsorption of Formaldehyde Molecule

The optimization of the $Me_{31}H_2CO$ adsorption complex gave one stable adsorption state irrespective of the metal and starting variants of location of the formaldehyde molecule on the surface; this state is characterized by a pronounced inclination of the molecular plane of H_2CO relative to the metal surface (the Me–C–O angle) (Fig. 1). According to the calculated values (Table 2), the slope of the molecular plane of H_2CO for adsorption on gold is ~20° larger than for adsorption on copper and silver. Earlier [22], three stable states of the H_2CO molecule were found for the Cu (111) face with close energies (within 3 kJ/mol). Two of these states are similar to the state obtained in this study and differ in the value of the Me–C–O angle (77.1° and 67.8°). In the third possible state, the molecular plane of H_2CO is perpendicular to the metal surface. This adsorption state of the formaldehyde molecule on the Au(111) surface was also found in [23], where the film model of the metal

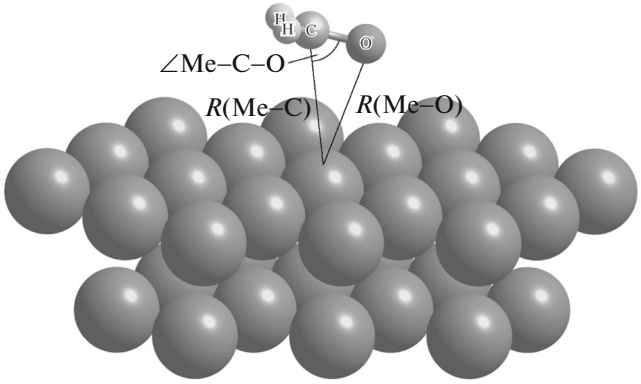

Fig. 1. Position of the formaldehyde molecule on the (111) face of IB metals corresponding to the stable state during adsorption from the gas phase.

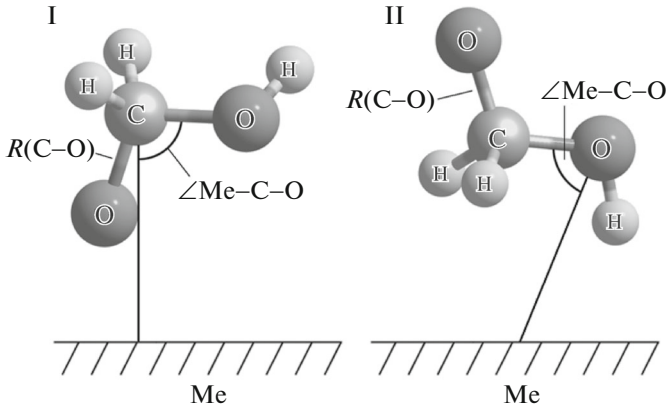

Fig. 2. Stable states of the methanediol anion on the (111) face.

surface was used; the calculated adsorption energy was 23.6 kJ/mol.

According to our calculations, the geometrical characteristics of the formaldehyde molecule do not change during its adsorption; the distance from the C and O atoms to the nearest metal atoms R(Me–O) and R(Me–C) is long enough. Taking into account the low adsorption energies and the nearly zero total charge Q of the adsorbed particle, we can conclude that the gas-phase adsorption of the formaldehyde molecule on the (111) face of IB metals is nonspecific. The adsorption energy obtained in this study for the Cu(111) surface agrees well with the similar values reported in [22]: –22.4, –22.9, and –24.8 kJ/mol for different adsorption sites of the H_2CO molecule.

Nondissociative Adsorption of the Methanediol Anion from the Gas Phase

The gas-phase adsorption of the methanediol anion was previously studied in [13]. Nevertheless, it is reasonable to cite the main results on both nondissociative and dissociative adsorption in more detailed form because below they are used in the analysis of liquid-phase adsorption.

Two stable adsorption states were found for the methanediol anion (Fig. 2). In state I, the $H_3CO_2^-$ anion is bonded with the metal surface via the oxygen atom that is close to the top position relative to the central atom of the surface of the Me_{31} cluster. In adsorption state II, the anion is bonded with the metal via three hydrogen atoms. For both adsorption states, a change in the geometry of the adsorbate particle is observed, namely, rotation of the OH group through a certain angle α relative to the C–O bond.

Adsorption state I is much more stable, especially for Cu and Ag, and is characterized by higher E_{ads} values compared with those of state II (Table 3). The adsorption energy of $H_3CO_2^-$ changes in the series: Au > Cu > Ag and Au > Ag ≈ Cu for adsorption states I and II, respectively. The high E_{ads} values suggest the specific interaction of the anion with the surface. The gold surface shows the highest activity with respect to the methanediol anion irrespective of the adsorption state.

The adsorption of the $H_3CO_2^-$, anion, in contrast to that of H_2CO, is accompanied by a distortion of the adsorbate geometry: an increase in the C–O bond length and a decrease in the C–H bond length compared with the value calculated for vacuum. The H–C–H angle, which is 103.9° in the isolated $H_3CO_2^-$ anion, increases during adsorption into state I, but does not change during adsorption into state II. The rotation of the OH group relative to the C–O bond during the adsorption of the methanediol anion was

Table 2. Characteristics of gas-phase adsorption of H_2CO

Me	R(C–O), pm	R(C–H), pm	H–C–H, deg	R(Me–O), pm	R(Me–C), pm	Me–C–O, deg	E_{ads}, kJ/mol	Q, au
–	120.7	110.0	115.4	–	–	–	–	0.000
Cu	121.4	110.8	116.1	295.7	312.4	70.8	–21.9	0.086
Ag	121.1	110.9	115.7	331.7	350.0	71.3	–11.1	0.058
Au	121.1	110.9	115.9	301.8	361.6	51.7	–14.9	0.087

characterized by the α angle, which was taken to be zero in the isolated ion. For adsorption state I, the α angle depends strongly on the nature of the metal (Cu > Ag > Au), while for state II the α angle is close to 180° for all the metals. The interatomic distances R(Me–O) and R(Me–C) indicate that the $H_3CO_2^-$ anion is closer to the metal surface during adsorption into state I, which is consistent with the higher E_{ads} values for this configuration. The Me–C–O angle is 74°–96° and changes in the series Cu > Au > Ag.

According to the results of calculations, the electron density transfer from the $H_3CO_2^-$ anion in state I to the metal is significant (Table 3), and the fraction of the transferred charge changes in the series Au > Cu > Ag. During adsorption of the methanediol anion into state II, the whole charge of the ion flows to the metal, and the total charge of the adsorbed ion is thus close to zero. The adsorbate charge does not correlate with the adsorption energy and the distances R(Me–O) and R(Me–C).

Dissociative Adsorption of the Methanediol Anion from the Gas Phase

According to the experimental data of [5, 6, 27–29], the methanediol anion on the copper and gold surface dissociates, under normal conditions, into the formate ion and two hydrogen atoms. The experimental studies of the electrooxidation of formaldehyde on gold [6] led to the following mechanism of the process:

$$H_3CO_2^- \rightleftharpoons H_2CO_2^- + H^\cdot, \quad (3)$$

$$H_2CO_2^- + OH^- \rightarrow HCOO^- + H_2O + e^-. \quad (4)$$

The adsorbed hydrogen atom formed at stage (3) is capable of further recombination or oxidation:

$$H^\cdot + H^\cdot \rightarrow H_2, \quad (5)$$

$$H^\cdot + OH^- \rightarrow H_2O + e^-. \quad (6)$$

The geometry optimization of the adsorbed complex corresponding to the dissociative state of the $H_3CO_2^-$ anion on the surface gave a single stable state (Fig. 3). The dissociation products are the formate ion and two hydrogen atoms. The $HCOO^-$ anion is adsorbed in the vertical orientation and is bonded with the metal surface via the oxygen atoms. The hydrogen atoms are adsorbed in the alveolar position. Tables 4 and 5 list the calculated parameters that characterize the dissociative adsorption of the $H_3CO_2^-$ anion from the gas phase.

The distance from the $HCOO^-$ anion to the metal surface was characterized by the distance R(Me–O), which is comparable to the corresponding value found for the nondissociative adsorption of the $H_2CO_2^-$ anion. The distances R(Me–O) and R(Me–C) change in the series Cu < Ag ≈ Ag. The C–H distance calculated for the isolated formate ion proved 4–5 pm higher than the corresponding value for the adsorbed particle. The C–O distance and the H–C–O angle change but slightly during the adsorption (Table 4). The Me–O–C angle is 121.6° and 121.7° in the case of adsorption on silver and gold, respectively, and 115.6° in the case of adsorption on copper.

Table 3. Characteristics of gas-phase adsorption of $H_3CO_2^-$ for adsorption states I and II

Me	R(C–O), pm	R(C–H), pm	H–C–H, deg	R(Me–O), pm	R(Me–C), pm	Me–C–O, deg	α, deg	E_{ads}, kJ/mol	Q, au
Vacuum	129.4	114.5	103.9	–	–	–	0.0	–	–1.000
Cu state I	136.7	110.6	107.3	220.6	297.9	82.6	171.1	–304.3	–0.299
Cu state II	131.1	113.4	103.5	383.0	348.8	96.0	170.8	–180.5	0.027
Ag state I	137.5	111.0	107.1	246.2	341.2	74.7	120.0	–276.7	–0.335
Ag state II	132.5	112.2	103.8	392.9	372.0	88.0	177.2	–184.9	0.018
Au state I	138.6	109.5	110.1	273.5	367.6	75.4	57.5	–334.9	–0.176
Au state II	132.6	112.3	103.3	394.0	362.8	92.1	179.2	–296.0	0.033

Table 4. Geometrical characteristics of gas-phase dissociative adsorption of $H_3CO_2^-$

Me	R(C–O), pm	R(C–H), pm	H–C–O, deg	R(Me–O), pm	Me–O–C, deg
–	125.4	115.4	114.5	–	–
Cu	125.7	110.7	116.6	206.0	115.6
Ag	125.8	111.4	115.5	234.0	121.6
Au	126.1	111.1	114.2	230.4	121.7

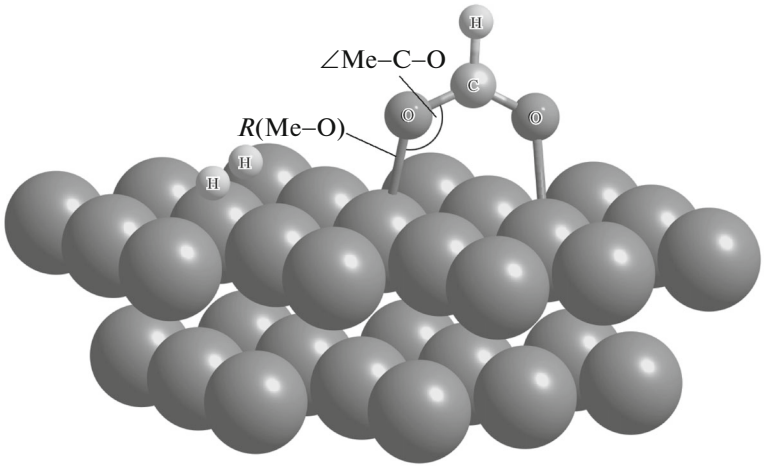

Fig. 3. Optimized geometry of the dissociated methanediol anion on the (111) face.

The dissociative adsorption energy of $H_3CO_2^-$ changes in the series Cu > Au > Ag, which does not agree with the dependence obtained for the case of nondissociative adsorption. The possibility of spontaneous dissociation of the $H_3CO_2^-$ anion on the (111) face of the metals in the gas phase can be evaluated from the sign of the dissociation energy, which was calculated as the difference between the dissociative and nondissociative adsorption energies:

$$E_{diss}(H_3CO_2^-) = E_{ads}(HCOO^- + 2H) - E_{ads}(H_3CO_2^-). \quad (7)$$

When calculating E_{diss}, we used the adsorption energies of nondissociated states I and II. The results are listed in Table 4. The negative values of $E_{diss}(H_3CO_2^-)$ for copper suggest the possibility of spontaneous dissociation of the methanediol anion on its surface, the initial state II being markedly preferable. For the same reason, dissociation of $H_3CO_2^-$ on the silver surface is energetically favorable only if the anion was initially in adsorption state II, though the probability of decomposition is now lower than on copper. For the gold (111) face, the calculation predicts that dissociation of the $H_3CO_2^-$ ion adsorbed from the gas phase is unlikely irrespective of the initial adsorption state.

It follows from the analysis of the value of the charge of the adsorbed particles (Table 5) that the electron density transfer from the $HCOO^-$ anion to the metal is large and comparable to the fraction of the transferred charge in the case of the adsorption of $H_3CO_2^-$, while the charge of H atoms on the surface is close to zero (Table 5). The small difference between the Q(H) values for two hydrogen atoms results from the effect of the $HCOO^-$ ion, which lies on the metal surface slightly asymmetrically relative to the H atoms.

Solvent Effect on the Adsorption of the Methanediol Anion

The adsorption of $H_3CO_2^-$ from aqueous solution can be described within the framework of the molecular model by the equation

$$Me_{31}(H_2O)_n + H_3CO_2^-(H_2O)_m \rightarrow [Me_{31}H_3CO_2(H_2O)_p]^- + (H_2O)_q. \quad (8)$$

A serious problem is to determine the structures of the reagents of (8). For this, it is necessary to determine the number of water molecules capable of being adsorbed as a monolayer on the cluster surface (n), the size of the first hydration shell of the adsorbed methanediol anion (m), and the number of water molecules in the adsorption complex capable of being accommo-

Table 5. Energy and charge characteristics of gas-phase dissociative adsorption of $H_3CO_2^-$; E_{diss}(I) and E_{diss}(II) are the dissociation energies from the starting adsorption states I and II, respectively

Me	$E_{ads,diss}$, kJ/mol	E_{diss}(I), kJ/mol	E_{diss}(II), kJ/mol	Q(HCOO$^-$), au	Q(H1), au	Q(H2), au
Cu	–326.4	–22.1	–181.9	–0.328	–0.097	–0.108
Ag	–195.0	81.7	–10.1	–0.398	–0.112	–0.116
Au	–248.2	86.7	47.8	–0.278	0.089	0.067

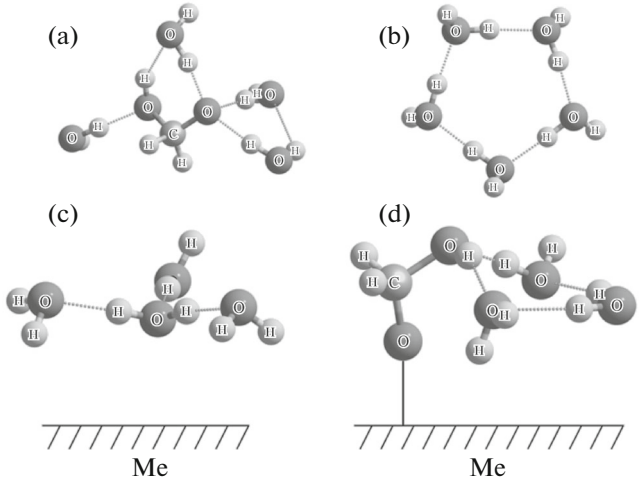

Fig. 4. Structures of reagents in processes (4) and (5): (a) $H_3CO_2^-$ $(H_2O)_4$, (b) $(H_2O)_5$, (c) $Me_{31}(H_2O)_4$, and (d) $[Me_{31}H_3CO_2(H_2O)_3]^-$.

dated on the Me_{31} cluster (p). The number of water molecules that passed in solution (q) during process (4) can be calculated by the material balance equation, assuming that $q = m + n - p$.

The preliminary calculations showed that the maximum number of water molecules capable of being adsorbed on the surface of the Me_{31} cluster m is 4. The first hydration shell of the $H_3CO_2^-$ anion also includes four water molecules. To determine p, calculations for a number of $[Me_{31}H_3CO_2(H_2O)_p]^-$ adsorption complexes with $p = 1$–6 were performed. It was found that at $p > 3$, the second hydration shell of the adsorbate particle starts to form, or one of the solvent molecules goes to the side surface of the cluster. Therefore, p was chosen to be 3, and, accordingly, $q = 5$. Equation (8) ultimately takes the form:

$$Me_{31}(H_2O)_4 + H_3CO_2^-(H_2O)_4 \rightarrow [Me_{31}H_3CO_2(H_2O)_3]^- + (H_2O)_5. \quad (9)$$

A similar model was used for the dissociative adsorption of $H_3CO_2^-$:

$$Me_{31}(H_2O)_4 + H_3CO_2^-(H_2O)_4 \rightarrow [Me_{31}(HCOO + 2H)(H_2O)_3]^- + (H_2O)_5. \quad (10)$$

The optimized structures of the reagents involved in reactions (9) and (10) are shown in Figs. 4 and 5. The same structure of adsorption and $Me_{31}(H_2O)_4$ complexes was found for all the three IB metals, with four water molecules forming an acyclic associate on the surface. For nondissociated adsorption of $H_3CO_2^-$, only one most favorable position of the anion on the surface (I) was considered. The structure of the $(H_2O)_5$ aqueous associate corresponding to the lowest total energy is cyclic, as reported earlier in [30, 31].

Table 6 shows the energy and charge characteristics of the adsorption of $H_3CO_2^-$ from aqueous solution. The results show that the energy of anion adsorption from the aqueous solution is much lower than from the gas phase. This is associated not only with the necessity of removing the water molecules from the surface and displacing the water molecules that are nearest to the adsorbed anion from their equilibrium positions, but also with partial dehydration of the adsorbate. The solvent effect also manifests itself in the fact that the dissociation of $H_3CO_2^-$ to the formate ion and two hydrogen atoms in aqueous solution is energetically favorable on all the metals under study, which corresponds to the picture observed experimentally [5]. Copper is the most surface-active metal in the cases of both dissociative and nondissociative adsorption of

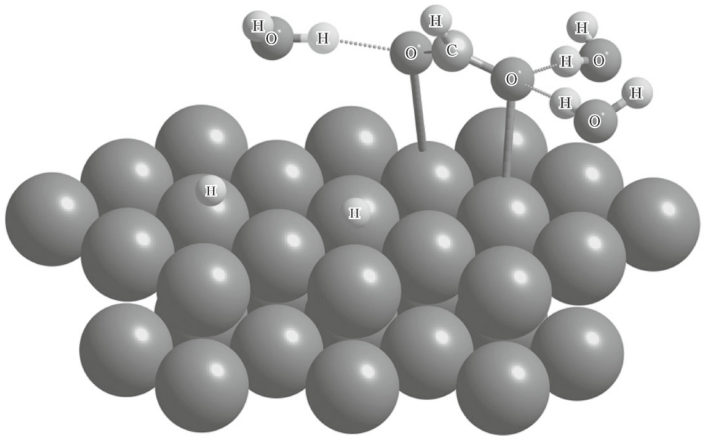

Fig. 5. Structure of the $[Me_{31}(HCOO + 2H)(H_2O)_3]^-$ adsorption complex.

Table 6. Energy and charge characteristics of the adsorption of $H_3CO_2^-$ from aqueous solution

Me	E_{ads}, kJ/mol	$E_{ads,diss}$, kJ/mol	E_{diss}, kJ/mol	$Q(H_3CO_2^-)$, au	$Q(HCOO^-)$, au
Cu	−116.6	−209.2	−92.6	−0.150	−0.112
Ag	−78.6	−103.8	−25.2	−0.107	−0.138
Au	−87.4	−107.8	−20.4	−0.059	−0.125

$H_3CO_2^-$, while silver is the least active. The fraction of the charge lost by the $H_3CO_2^-$ and $HCOO^-$ anions during adsorption from the aqueous solution is higher than during adsorption from the gas phase because in aqueous solution, the charge flows from the anion not only to the metal, but also to the nearest solvent molecules.

CONCLUSIONS

1. The formaldehyde molecule is adsorbed from the gas phase on Group IB metals physically, while the methanediol anion is adsorbed specifically. The spatial structure of H_2CO does not change, while the structure of $H_3CO_2^-$ changes appreciably, which primarily shows itself in a change in the interatomic bond length, which increases for C–O and decreases for C–H.

2. The $H_3CO_2^-$ anion can exist on the surface of IB metals in two stable adsorption states, which differ in the character of the bond with the metal atoms: via the oxygen atom, or via three hydrogen atoms. The first state is energetically more favorable; the adsorption energy changes in the series Au > Cu > Ag; the fraction of the charge transferred from anion to metal during adsorption decreases in the same order.

3. In the aqueous solution, spontaneous dissociation of the methanediol anion into the formate ion and two hydrogen atoms is possible on all the IB metals, while in the gas phase, the $H_3CO_2^-$ anion can dissociate only on the copper surface.

4. The $HCOO^-$ anion bonded by the metal surface via the oxygen atoms is orientated vertically. The C–O bond length and the O–C–H angle during the gas-phase adsorption of the formate ion do not change; the O–C–O angle, which is almost the same for Ag and Au, markedly decreases on passing to Cu, correlating with the decrease in the interatomic distance in the cluster.

5. The adsorption of $H_3CO_2^-$ and $HCOO^-$ anions is accompanied by a considerable charge transfer to the metal. In the aqueous solution, the anions that lie on the surface lose a considerably larger part of their charge than in the gas phase.

ACKNOWLEDGMENTS

This study was financially supported by the Ministry of Education and Science within the framework of state assignment for higher educational institutions in the field of research activities for 2014-2016 (project no. 675).

REFERENCES

1. K. Kiler, Adv. Catal. **31**, 243 (1982).
2. J. F. Walker, *Formaldehyde* (Reinhold, New York, 1944; Goskhimizdat, Moscow, 1957).
3. S. K. Ogorodnikov, *Formaldehyde* (Khimiya, Moscow, 1984) [in Russian].
4. R. Parsons and T. van der Noot, J. Electroanal. Chem. **257**, 9 (1988).
5. L. A. Mikhnenko, N. B. Morozova, V. A. Zinov'eva, and A. V. Vvedenskii, Kondens. Sredy Mezhfaz. Granitsy **7**, 55 (2005).
6. M. V. ten Kortenaar, Z. I. Kolar, J. J. M. de Goeij, and G. Frens, Langmuir **18**, 10279 (2002).
7. S. Titmuss, A. Wander, and D. A. King, Chem. Rev. **96**, 1291 (1996).
8. S. N. Lanin, Yu. G. Polynskaya, D. A. Pichugina, V. Nguen, A. V. Beletskaya, N. E. Kuz'menko, and A. F. Shestakov, Russ. J. Phys. Chem. A **87**, 1520 (2013).
9. Y. A. Elfimova, D. A. Pichugina, I. A. Anan'eva, A. G. Mazhuga, and O. A. Shpigun, Russ. J. Phys. Chem. A **86**, 1623 (2012).
10. D. A. Pichugina, S. N. Lanin, A. V. Beletskaya, A. A. Bannykh, A. A. Peristyi, M. V. Polyakova, and N. E. Kuz'menko, Russ. J. Phys. Chem. A **86**, 1892 (2012).
11. N. A. Rogozhnikov, Russ. J. Electrochem. **49**, 1031 (2013).
12. An. M. Kuznetsov, A. N. Maslii, and M. S. Shapnik, Russ. J. Electrochem. **36**, 1303 (2000).
13. S. S. Starodubov, I. V. Nechaev, and A. V. Vvedenskii, Sorbtsion. Khromatogr. Protsessy **14**, 296 (2014).
14. J. Emsley, *The Elements* (Clarendon, Oxford, 1991).
15. A. D. Becke, J. Chem. Phys. **98**, 1372 (1993).
16. M. J. Frisch et al., *Gaussian 03,* Rev. C.02 (Gaussian Inc., Pittsburgh, 2003).
17. V. A. Rassolov, J. A. Pople, M. A. Ratner, and T. L. Windus, J. Chem. Phys. **109**, 1223 (1998).
18. W. R. Wadt and P. J. Hay, J. Chem. Phys. **82**, 284 (1985).
19. M. D. Morse, Chem. Rev. **86**, 1049 (1986).

20. *Molecular Constants of Inorganic Compounds*, Ed. by K. S. Krasnov (Khimiya, Leningrad, 1979) [in Russian].
21. A. I. Volkov and I. M. Zharskii, *Large Chemical Reference Book* (Sovrem. Shkola, Minsk, 2005) [in Russian].
22. J. R. B. Gomes, J. A. N. F. Gomes, and F. Illas, J. Mol. Catal. A: Chem. **170**, 187 (2001).
23. W.-K. Chen et al., J. Mol. Struct. (THEOCHEM) **770**, 87 (2006).
24. H. B. Schlegel, J. Comput. Chem. **3**, 214 (1982).
25. An. M. Kuznetsov, A. N. Maslii, and L. I. Krishtalik, Russ. J. Electrochem. **44**, 34 (2008).
26. R. S. Mulliken, J. Chem. Phys. **36**, 3428 (1962).
27. Z. Jusys, J. Electroanal. Chem. **375**, 257 (1994).
28. M. V. ter Kortenaar, C. Tessont, Z. I. Kolar, and H. van der Weijde, J. Electrochem. Soc. **146**, 2146 (1999).
29. M. V. ter Kortenaar, Z. I. Kolar, J. J. M. de Goeij, and G. Frens, J. Electrochem. Soc. **148**, E327 (2001).
30. J. D. Bene and J. A. Pople, J. Chem. Phys. **52**, 4858 (1970).
31. M. F. Vernon et al., J. Chem. Phys. **77**, 47 (1982).

Translated by L. Smolina